

DVCS on a virtual pion at EIC and EICC

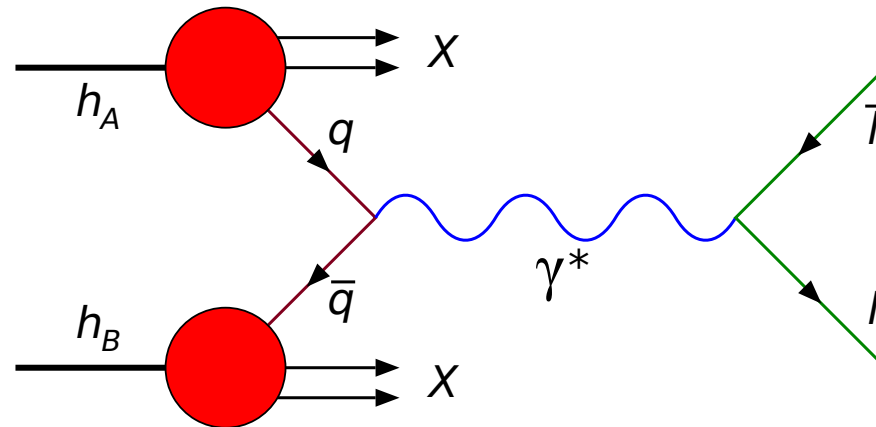


The pion structure

- The pion is a much simpler object than the proton (2 GPDs vs 8 GPDs):
=> Non-perturbative techniques improved and models of Form Factors/PDFs and now GPDs can be computed.
- Although theoretically easier, experimentally it is challenging to probe its inner structure.

PDF accessed with Drell-Yan

- Impinging a pion beam onto a proton target like in COMPASS experiment, one can access the PDF of the pion via Drell-Yan.



- But accessing the pion structure with an electron beam would require a luminosity unreachable with pion beams.

The Sullivan process

- It was noticed that in the final state of electron scattering events, a nucleon was « surviving » with a low momentum transfer :
The virtual photon is interacting with the meson cloud.

PHYSICAL REVIEW D

VOLUME 5, NUMBER 7

1 APRIL 1972

One-Pion Exchange and Deep-Inelastic Electron-Nucleon Scattering

J. D. Sullivan*

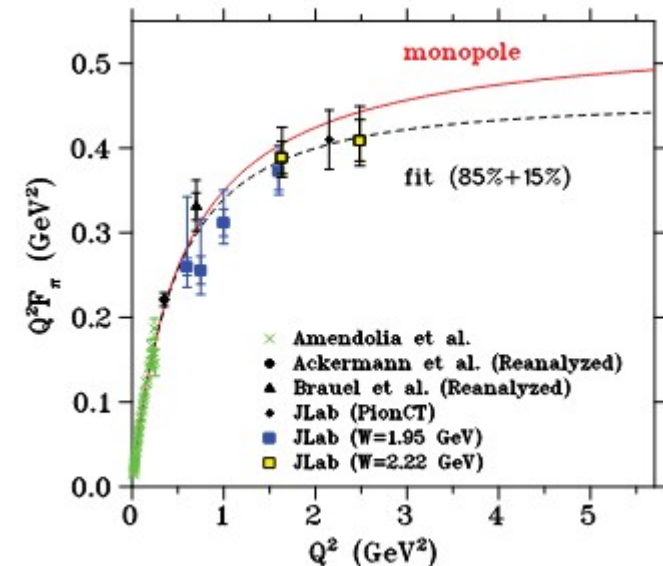
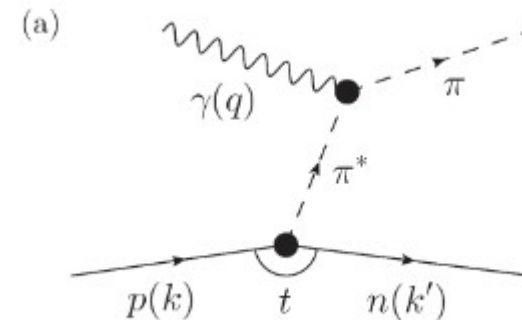
National Accelerator Laboratory, Batavia, Illinois 60510

(Received 29 November 1971)

The role of one-pion exchange is examined in the deep-inelastic region for electron-nucleon scattering. Exclusive channels like πN , $\pi\Delta$ will contribute negligible, nonscaling contributions to σ_S . On the other hand, inclusive final states like $N + \text{"anything,"}$ where the detected final nucleon is slow in the lab system, afford the opportunity to experimentally determine the structure functions for electron-pion scattering provided the characteristic one-pion-exchange structure (dip or peak) is observed at small momentum transfer.

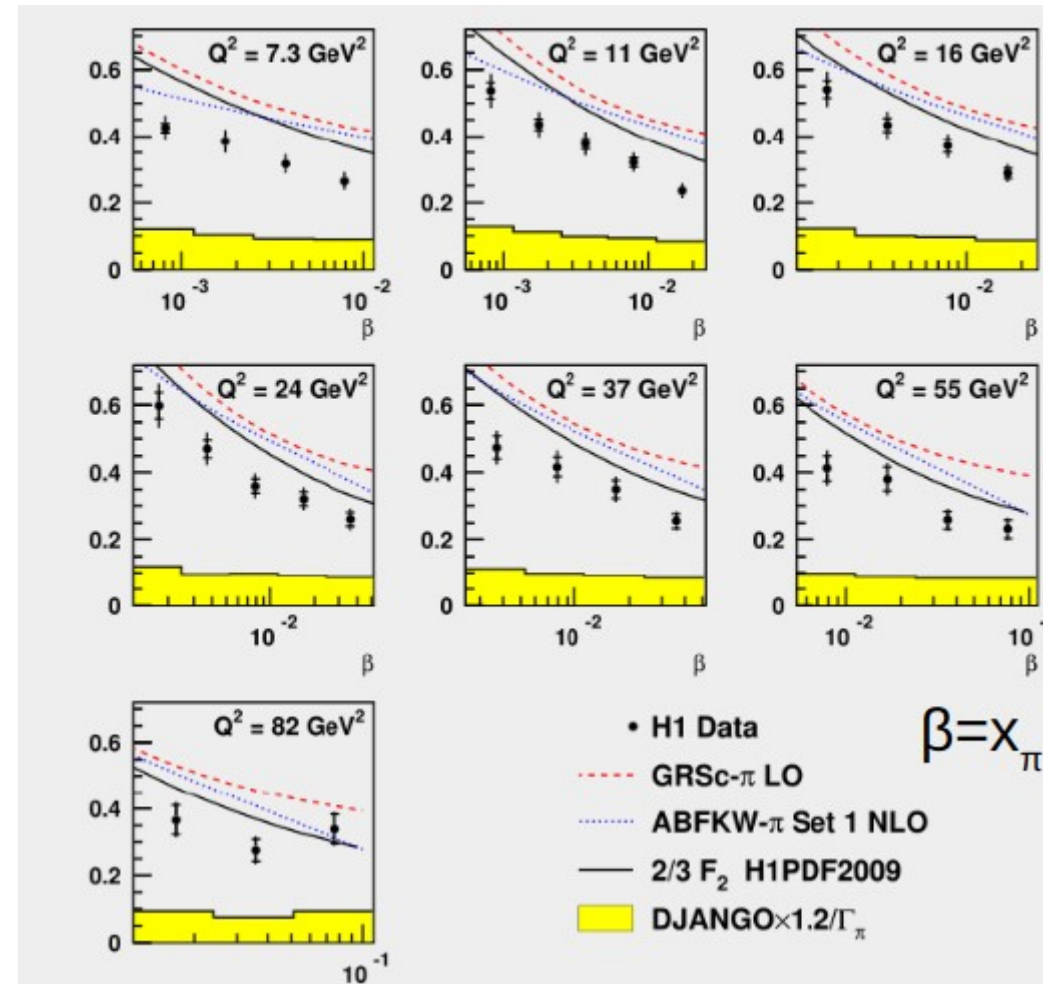
Form Factors at large momentum transfer

- By measuring $ep \rightarrow e n \pi^+$, one can access the pion form factor.
- With t -low enough, the process can be seen as a Sullivan process.
- Now, experimentally, the measurement is quite complicated because it requires a Rosenbluth separation (Only through the longitudinal cross section).



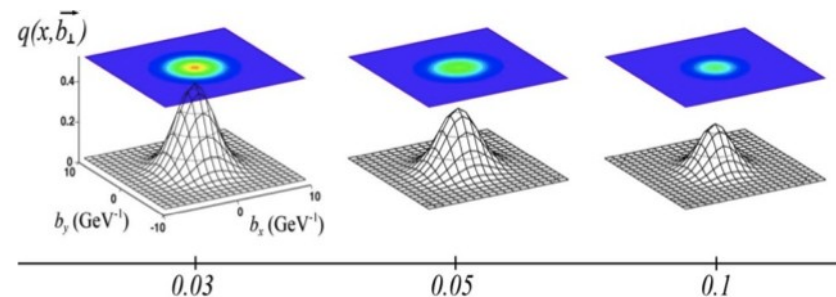
PDFs through Sullivan process

- Same idea as the form factors however the final state is « unconstrained » apart from detecting a recoil nucleon with low-momentum transfer t .
- First measurement at HERA.
- Conditionnally approved experiment in Hall A, and as well feasible to EIC.



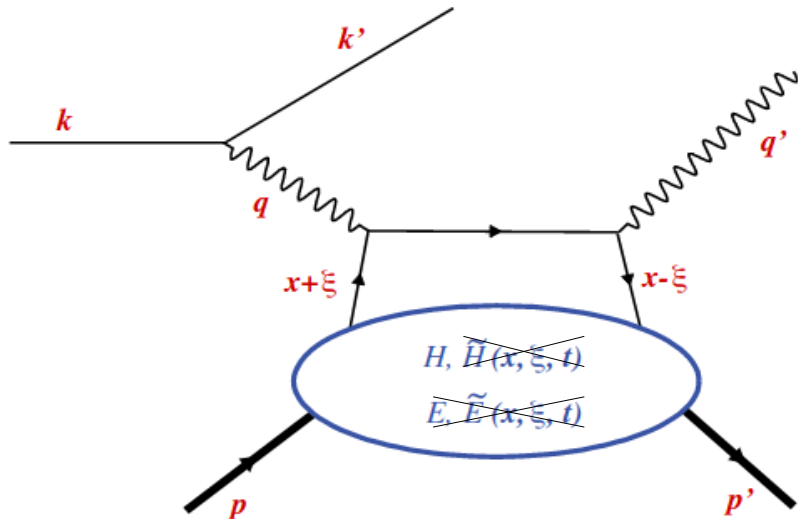
But are GPDs accessible via Sullivan process ?

- GPD : Generalized parton distributions.
It provides correlation between longitudinal momentum and transverse position of partons in a hadron.



- It is accessible via exclusive processes, with a final state completely determined.

Deeply virtual compton scattering



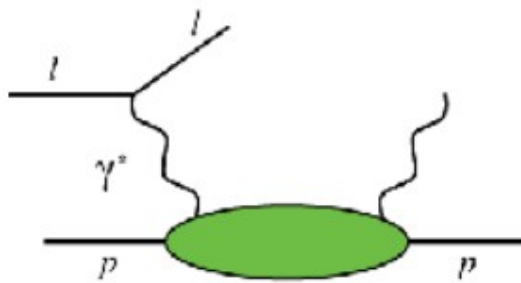
- $Q^2 = -q^2 = -(k - k')^2$.
- $x_B = \frac{Q^2}{2p \cdot q}$
- x longitudinal momentum fraction carried by the active quark.
- $\xi \sim \frac{x_B}{2-x_B}$ the longitudinal momentum transfer.
- $t = (p - p')^2$ squared momentum transfer to the nucleon.

The GPDs enter the DVCS amplitude through a complex integral. This integral is called a *Compton form factor* (CFF).

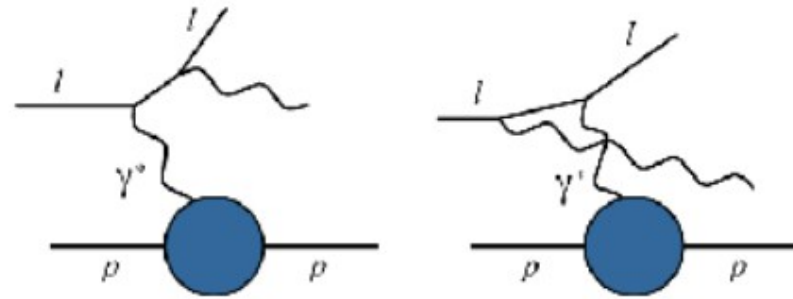
$$\mathcal{H}(\xi, t) = \int_{-1}^1 H(x, \xi, t) \left(\frac{1}{\xi - x - i\epsilon} - \frac{1}{\xi + x - i\epsilon} \right) dx .$$

Photon Electroproduction

Experimentally we measure the cross section of the process $ep \rightarrow ep\gamma$.



DVCS



Bethe-Heitler

The measured cross section is the coherent sum of both amplitudes :

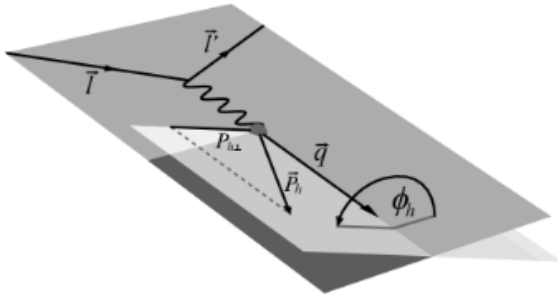
- Here an interference term appears and offers unique opportunity to access both real and imaginary parts of CFF.

$$\frac{d^5\sigma^{e\pi \rightarrow e\gamma\pi}(\lambda, \pm e)}{dy_\pi dx_B^\pi dt_\pi d\phi d\phi_e} = \frac{d^2\sigma_0}{dQ^2 dx_B^\pi} \frac{1}{e^6} \times \left[|\mathcal{T}^{BH}|^2 + |\mathcal{T}^{DVCS}|^2 \mp \mathcal{I} \right],$$

$$\frac{d^2\sigma_0}{dQ^2 dx_B^\pi} = \frac{\alpha_{\text{QED}}^3 x_B^\pi y_\pi}{16\pi^2 Q^2 \sqrt{1 + \epsilon^2}},$$

$$\epsilon^2 = 4m_\pi^2 (x_B^\pi)^2 / Q^2,$$

Harmonic structure of the cross section



We can partially unfold the contributions, studying the ϕ -dependence.

$$|\mathcal{T}^{BH}|^2 = \frac{e^6 \sum_{n=0}^2 c_n^{BH} \cos(n\phi)}{x_B^2 t y^2 (1 + \epsilon^2)^2 \mathcal{P}_1(\phi) \mathcal{P}_2(\phi)} \quad \leftarrow \text{KNOWN!}$$

$$|\mathcal{T}^{DVCS}|^2 = \frac{e^6}{y^2 Q^2} \left\{ c_0^{DVCS} + \sum_{n=1}^2 \left[c_n^{DVCS} \cos(n\phi) + \lambda s_1^{DVCS} \sin(n\phi) \right] \right\}$$

$$\mathcal{J} = \frac{e^6}{x_B y^3 \mathcal{P}_1(\phi) \mathcal{P}_2(\phi) t} \left\{ c_0^{\mathcal{J}} + \sum_{n=1}^3 \left[c_n^{\mathcal{J}} \cos(n\phi) + \lambda s_n^{\mathcal{J}} \sin(n\phi) \right] \right\}$$

Accessing the CFF

The CFFs are encapsulated in c_n and s_n , offering a parameterization of the cross section. In the leading twist approximation for unpolarized target:

$$c_0^{DVCS} \propto \mathcal{C}^{DVCS}(\mathcal{F}, \mathcal{F}^*) = 4(1 - x_B)\mathcal{H}\mathcal{H}^* + \dots \quad (1)$$

$$c_1^J \propto \text{Re } \mathcal{C}^J(\mathcal{F}) = F_1 \text{Re}\mathcal{H} + \xi(F_1 + F_2) \text{Re}\tilde{\mathcal{H}} - \frac{t}{4M^2} F_2 \text{Re}\mathcal{E},$$

$$s_1^J \propto \text{Im } \mathcal{C}^J(\mathcal{F}) = F_1 \text{Im}\mathcal{H} + \xi(F_1 + F_2) \text{Im}\tilde{\mathcal{H}} - \frac{t}{4M^2} F_2 \text{Im}\mathcal{E},$$

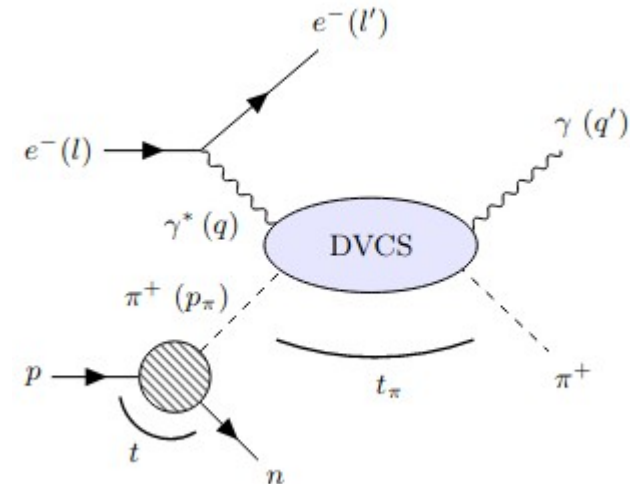
- As already mentioned earlier, the pion has only the GPD $H \Rightarrow$ the unique CFF is constrained by only playing with the beam polarization.

Related Articles

- Articles used for experimental study :
 - EICC white paper Frontiers of Physics, Volume 16 Issue (6):64701, 2021
 - EIC Yellow report <https://arxiv.org/abs/2103.05419>
- Articles used for theory :
 - Morgado Chavez et al.,**
Pion GPDs: A path toward phenomenology, arXiv 2110.06052
 - Belitsky, Muller Phys.Rev.D 79:014017, 2009
 - Amrath et al. Eur.Phys.J.C 58:179-192, 2008

Sullivan DVCS

- DVCS depends on 4 kinematical variables :
 Q^2 , x_B/y , t_π , ϕ .
- For Sullivan DVCS, we need two additional variables to characterize the virtual pion :
 - t : momentum transfer to nucleon
 - x_π : the energy fraction carried by the pion in the ep com-frame.
- The total cross section will be the product of the DVCS cross section and a virtual pion flux depending on t and x_π .



$$\frac{d^8 \sigma^{\text{Sul}}(\lambda, \pm e)}{dy dQ^2 dt_\pi d\phi d\phi_e dt dx_\pi d\phi_n} = x_\pi \frac{g_{\pi NN}^2}{16\pi^3} F(t)^2 \frac{-t}{(m_\pi^2 - t)^2} |J_{x_B^\pi}^{Q^2}| \frac{d^5 \sigma^{e\pi \rightarrow e\gamma\pi}(\lambda, \pm e)}{dy_\pi dx_B^\pi dt_\pi d\phi d\phi_e}$$

Regarding the event generation

1) First we generate the virtual pion :

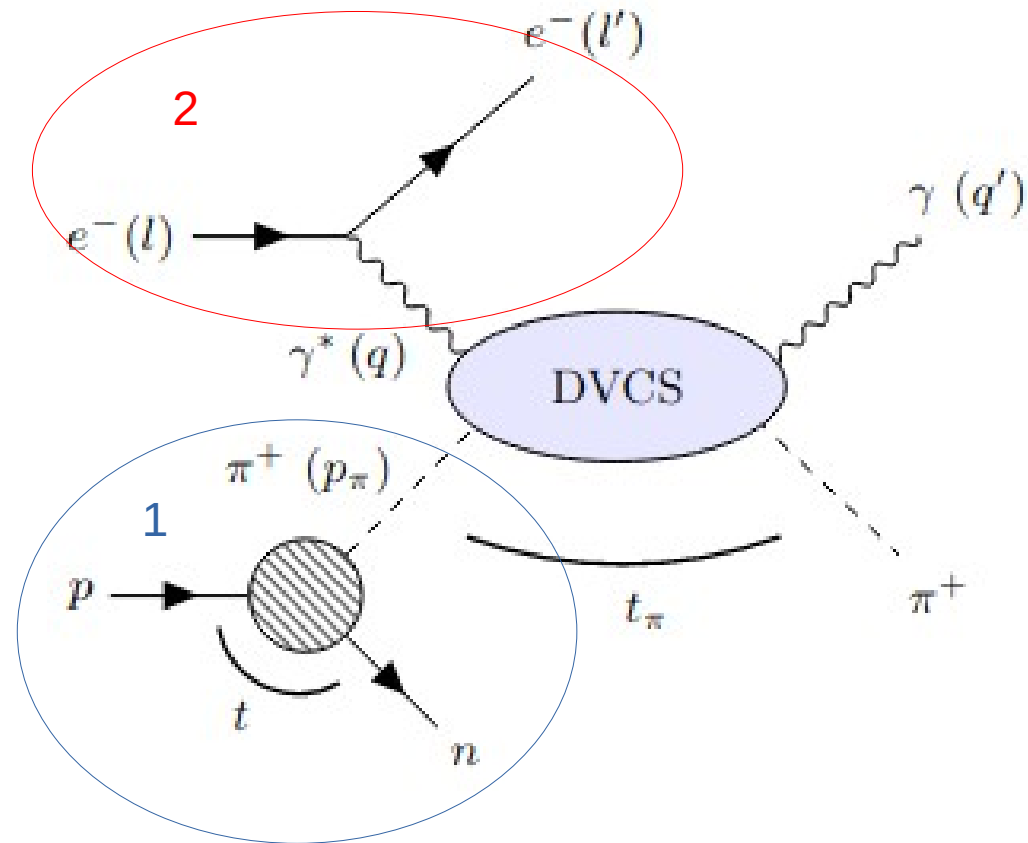
- t uniformly in $[-0,6 ; 0]$,
- x_{π} in a depending on t ,
- and ϕ_N , rotation around proton axis.

2) Then the virtual photon is generated with :

- Q^2 in $[1 ; 100] \text{ GeV}^2$
- y depending on Q^2
- ϕ_e , rotation around virtual photon axis

3) Once both virtual pion and photons are characterized, then t_{π} in $[-0,6 ; 0]$ and ϕ are generated.

Events are then weighted by the cross section and a phase space factor.



The electron ion collider

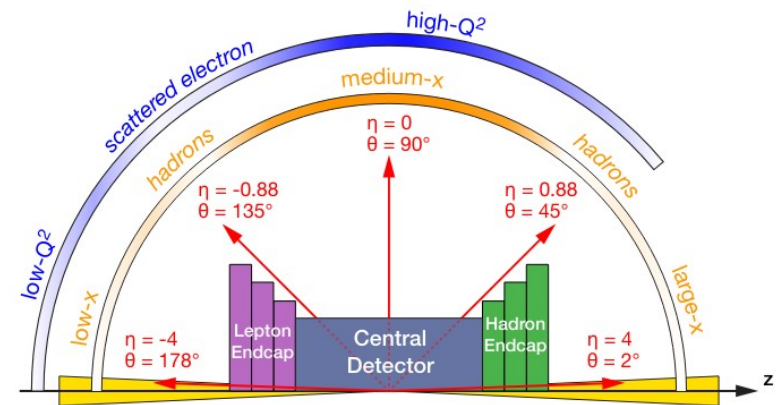
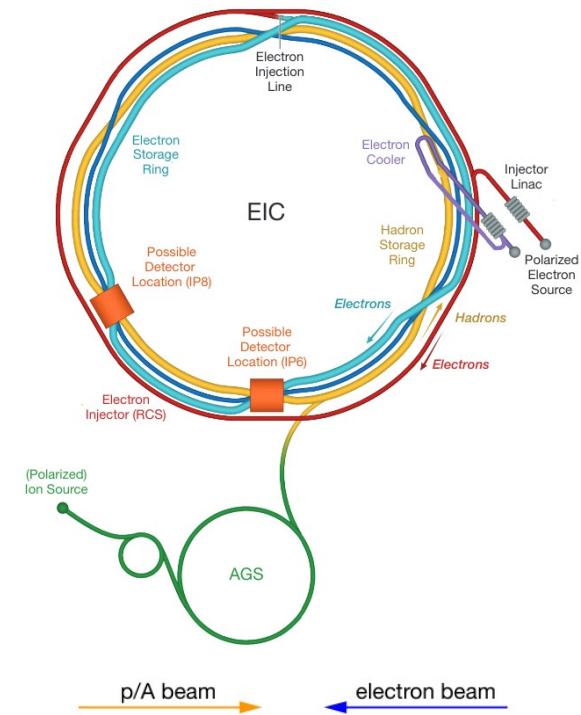
The electron-ion collider will be located in Brookhaven National Laboratory.

It will offer longitudinally polarized electron beam and transversely polarized protons.

Beams	Collision energy modes (GeV)							
	E_e	E_h	E_e	E_h	E_e	E_h	E_e	E_h
$e+p$	18	275	10	100	5	100	5	41

For our studies, we used a Toy geometry of the detector :

- Photon detected for $|\eta| < 4$.
- Electron detected and identified for $|\eta| < 3,5$.
- Neutron detected in the ZDC if $\theta < 5,5$ mrad.
- Pion detected either if $|\eta| < 4$ or θ between 6 and 20 mrad.



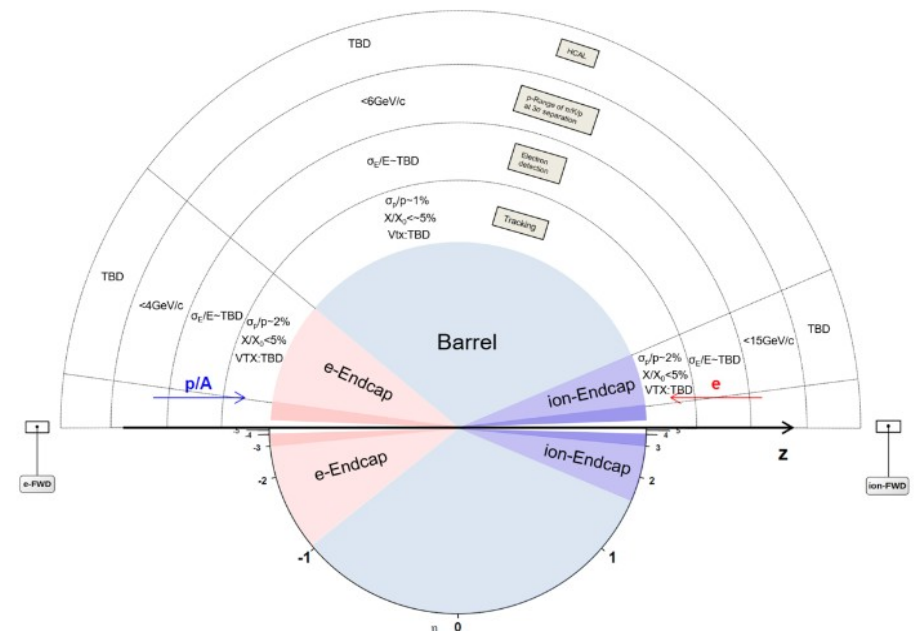
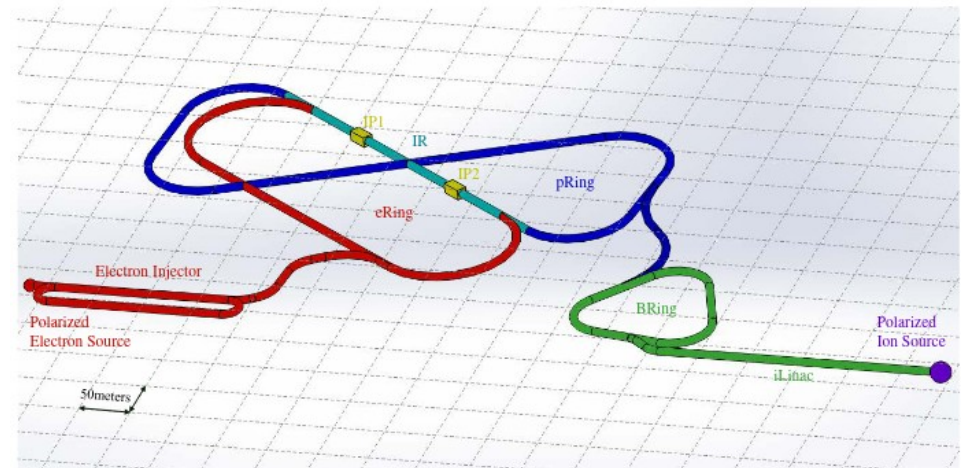
The electron ion collider in China

-There is a project to build an electron-ion collider facility in China, un an upgrade of the HIAF facility.

-Electron energy will be 3,5 GeV while proton energy will reach up to 20 GeV : More ideal to access valence region.

-The electron longitudinal polarization will reach 80 % and an expected luminosity of 50 fb-1 / year.

-For our study, we considered almost same geometry as for EIC except for the neutron calorimeter : No information is provided in the white paper.
=> Ideal detection of the neutron.

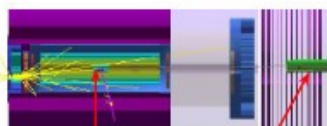


Detector Layout

proton

electron

Electron
Photon
Pion



IP

B0 sensors:
Rin ~ 3.4 cm
Rout ~ 20 cm
50x50 μm^2 pixel pitch

Zpos = 5.9 m
Xpos = 15 cm

Pion

~~**Off momentum tracker:**
Rin ~ 10 *cm (?),
10x30cm
500x500 μm^2 pixel pitch~~

~~Zpos = 22.5 m
Xpos = 75 cm~~

~~**Roman Pots:**
Rin ~ 10σ
20x10 cm^2
500x500 μm^2 pixel pitch~~

~~Zpos = 26.2 m
Xpos = 82 cm~~

~~**RP2 (not seen):**
Zpos = 28.2 m
Xpos = 91 cm~~

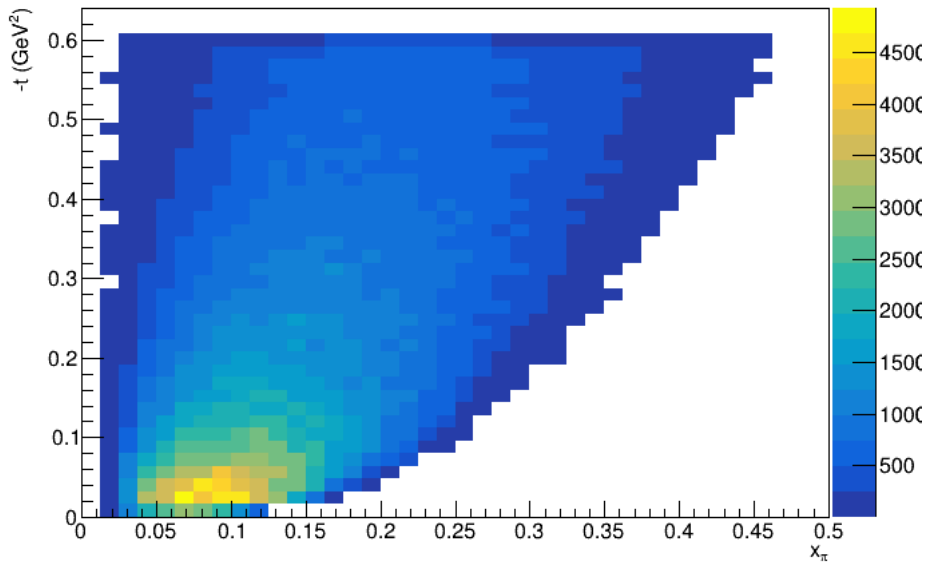
ZDC:
60x60cm EMCAL
LG: 1x1 cm^2
HG: 100x100 μm^2
HCAL: 10x10 cm

Zpos = 38 m
Xpos = 90 cm

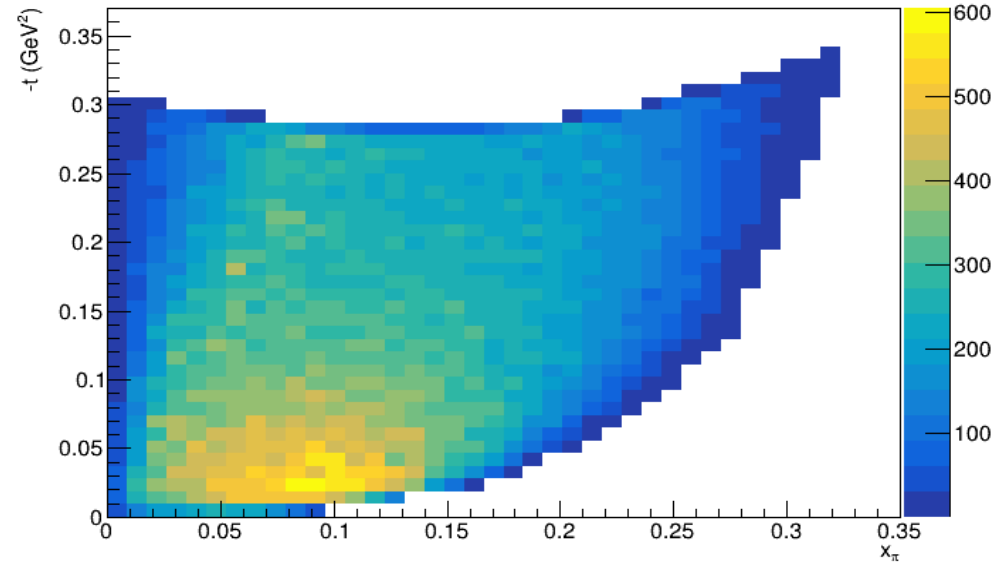
Neutron

Kinematics : t and x_{π}

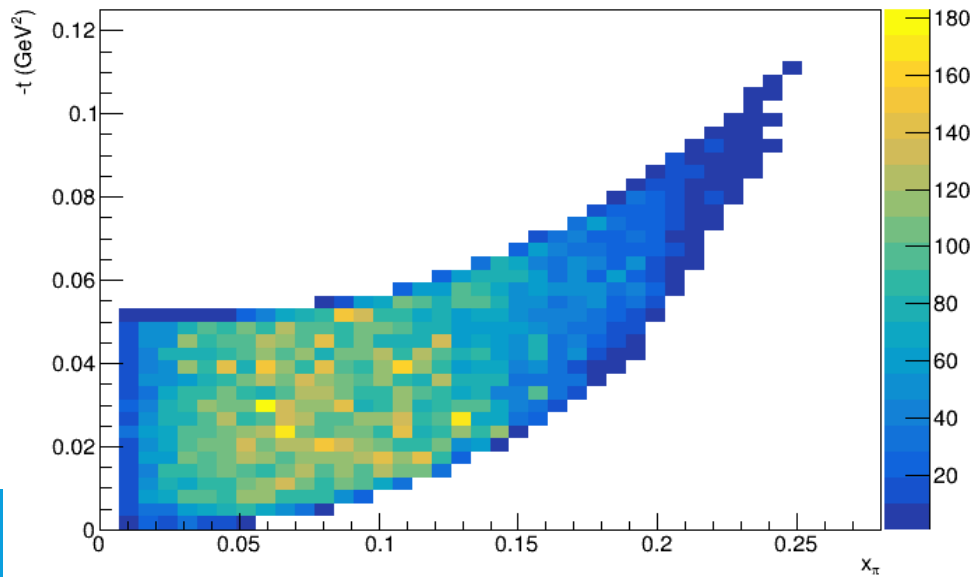
$-t$ vs x_{π} , $s=3 \times 20$, 10 fb^{-1}



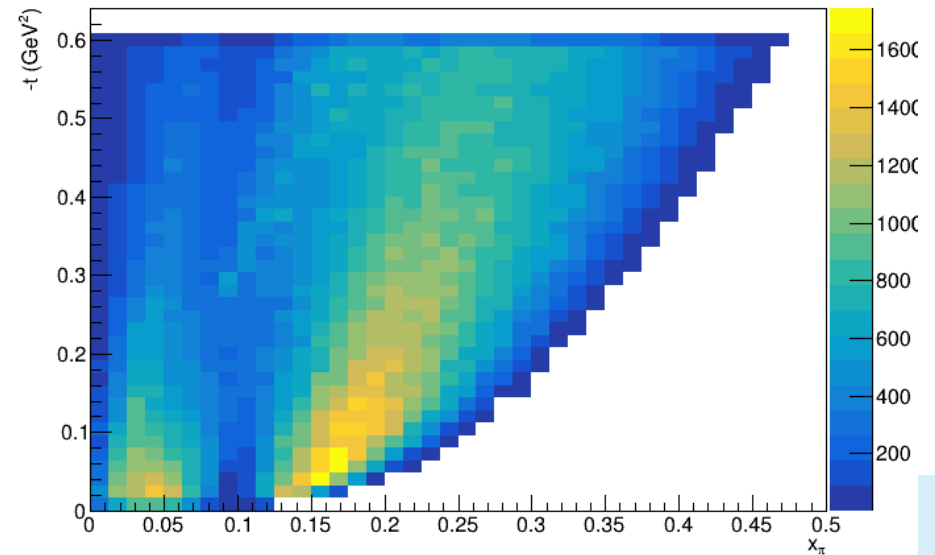
$-t$ vs x_{π} , $s=10 \times 100$, 10 fb^{-1}



$-t$ vs x_{π} , $s=5 \times 41$, 10 fb^{-1}

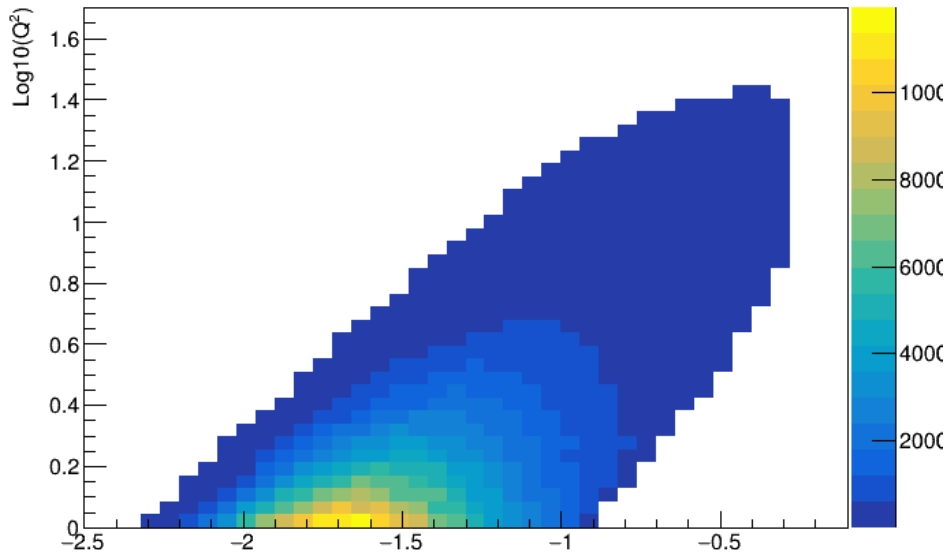


$-t$ vs x_{π} , $s=18 \times 275$, 10 fb^{-1}

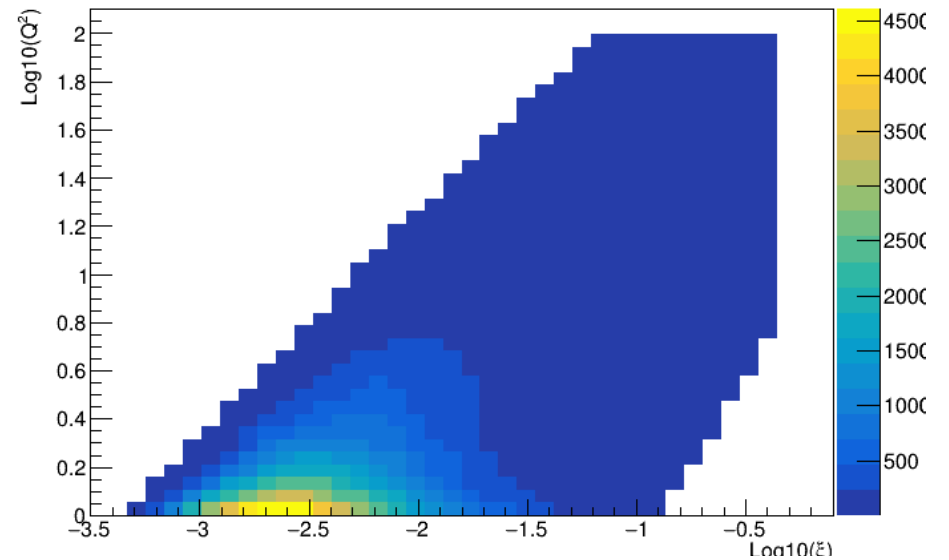


Kinematics : Q^2 and ξ

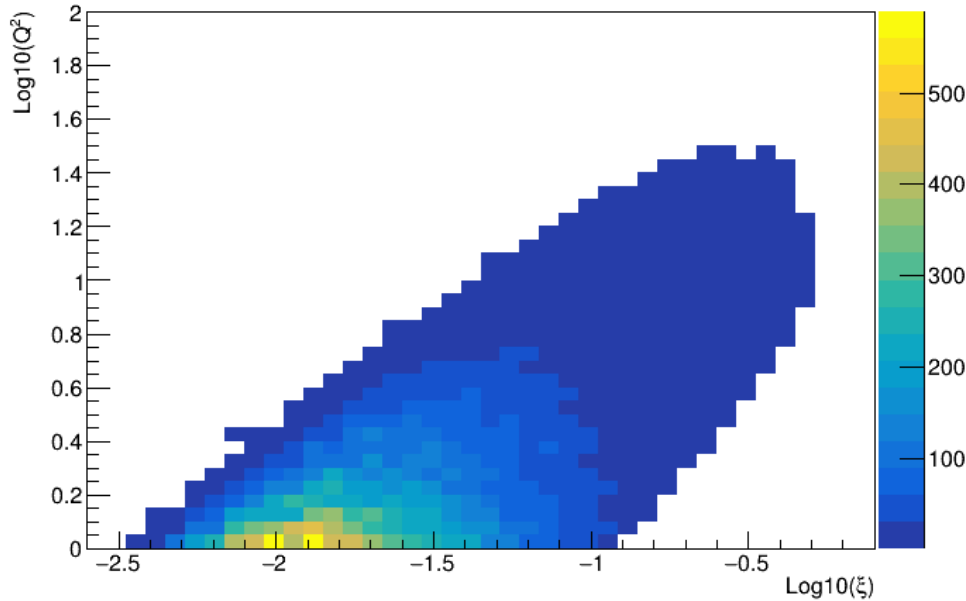
Log10(ξ) vs Log10(Q^2), $s=3 \times 20$, 10 fb-1



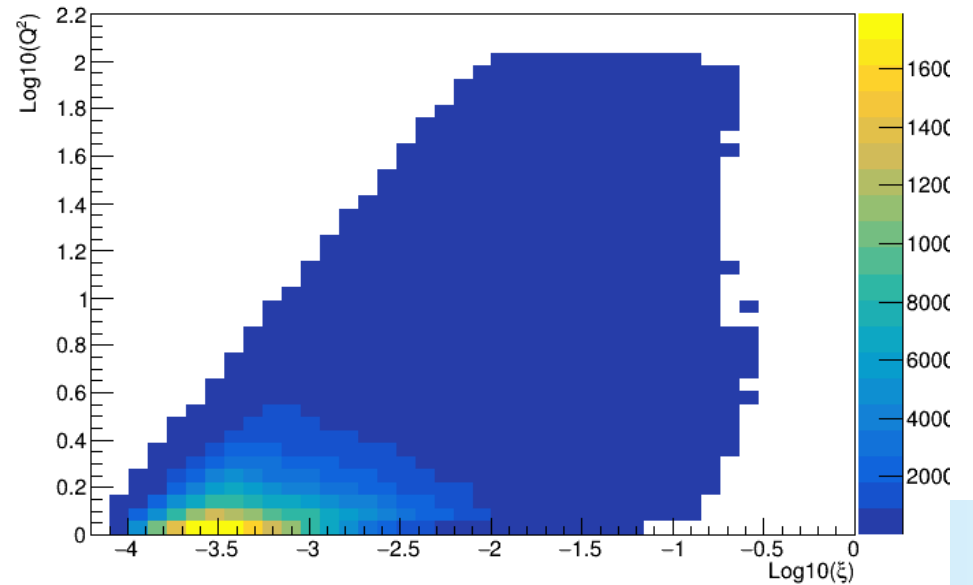
Log10(ξ) vs Log10(Q^2), $s=10 \times 100$, 10 fb-1



Log10(ξ) vs Log10(Q^2), $s=5 \times 41$, 10 fb-1

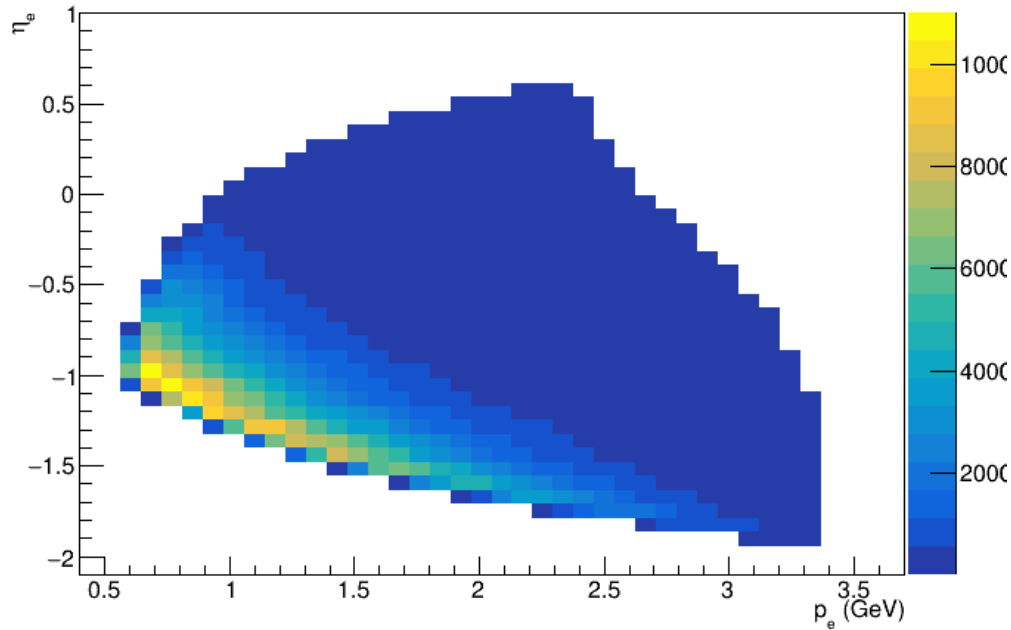


Log10(ξ) vs Log10(Q^2), $s=18 \times 275$, 10 fb-1

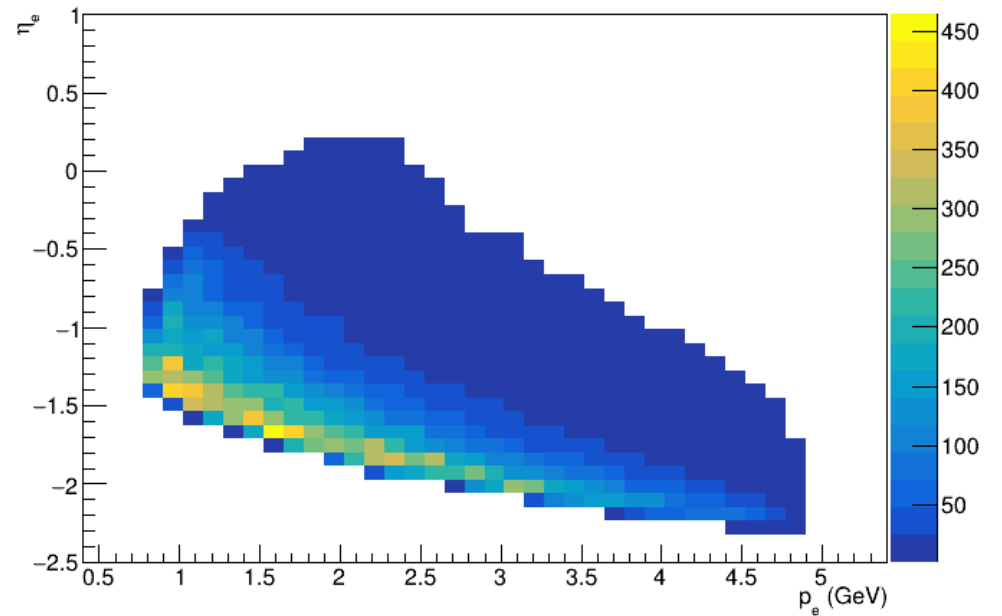


Electron distributions

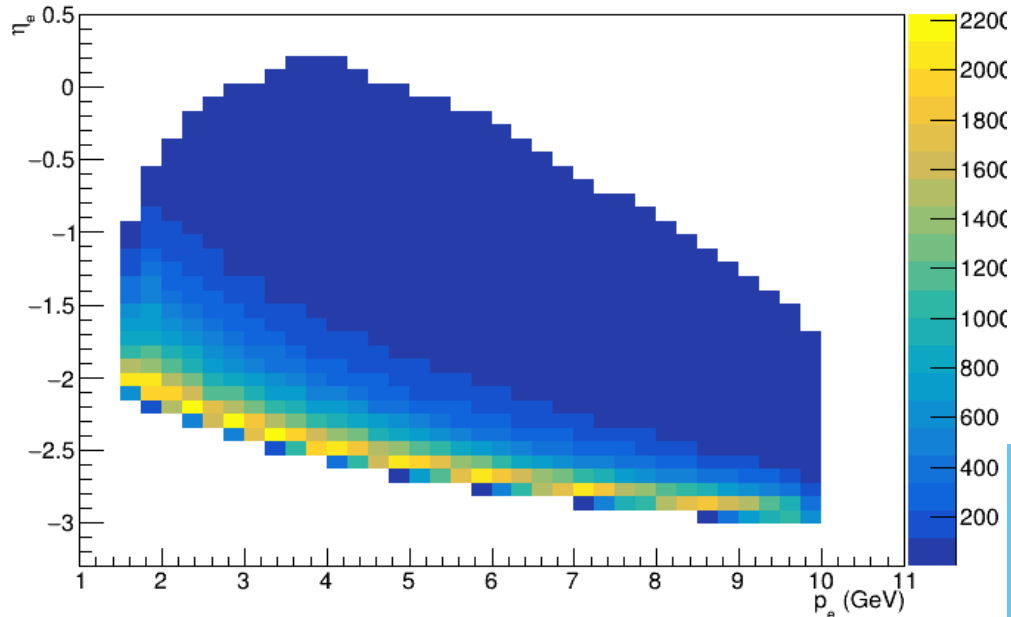
η_e vs p_e , $s=3 \times 20$, 10 fb-1



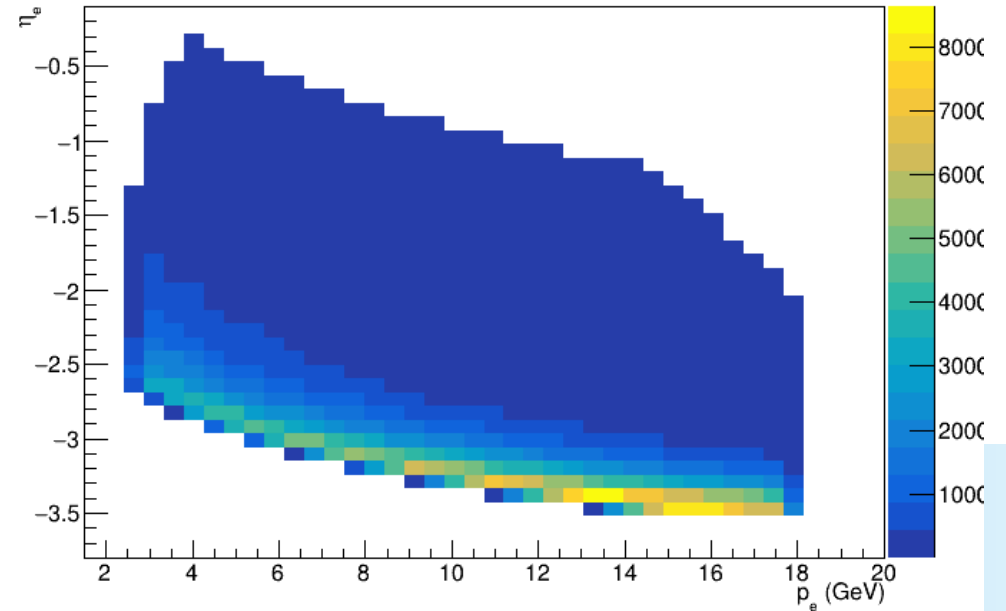
η_e vs p_e , $s=5 \times 41$, 10 fb-1



η_e vs p_e , $s=10 \times 100$, 10 fb-1

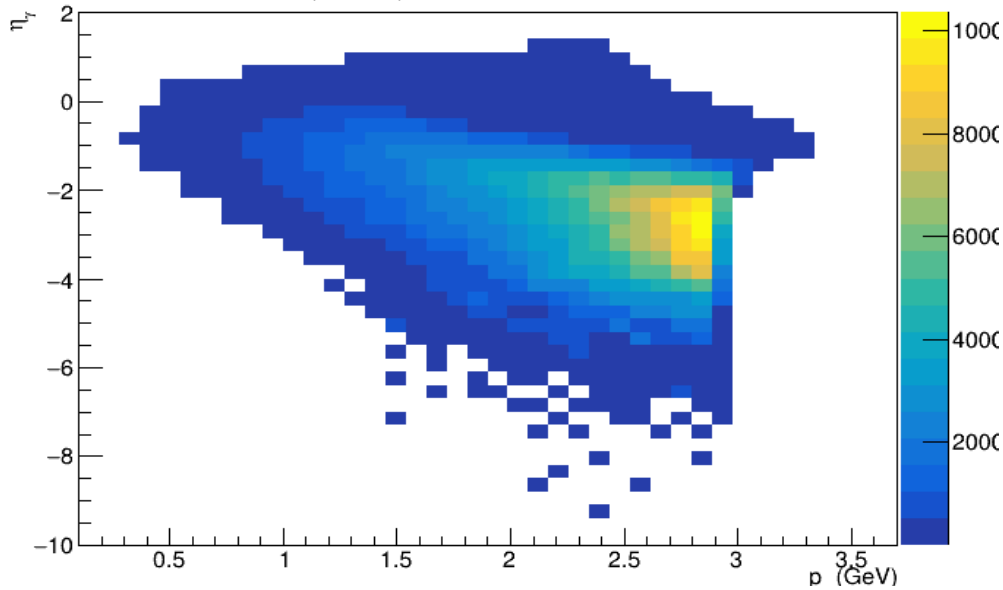


η_e vs p_e , $s=18 \times 275$, 10 fb-1

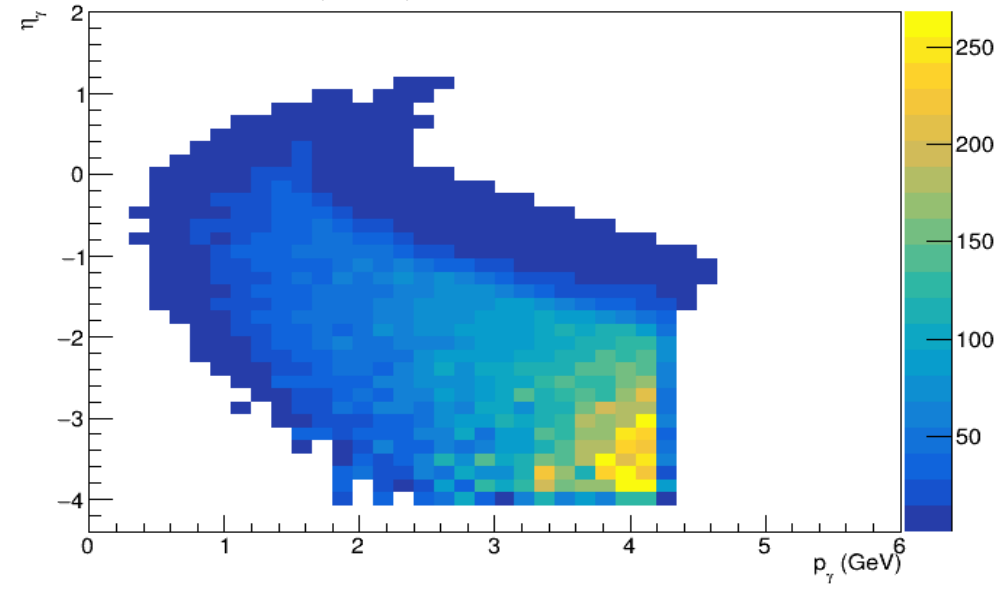


Photon distributions

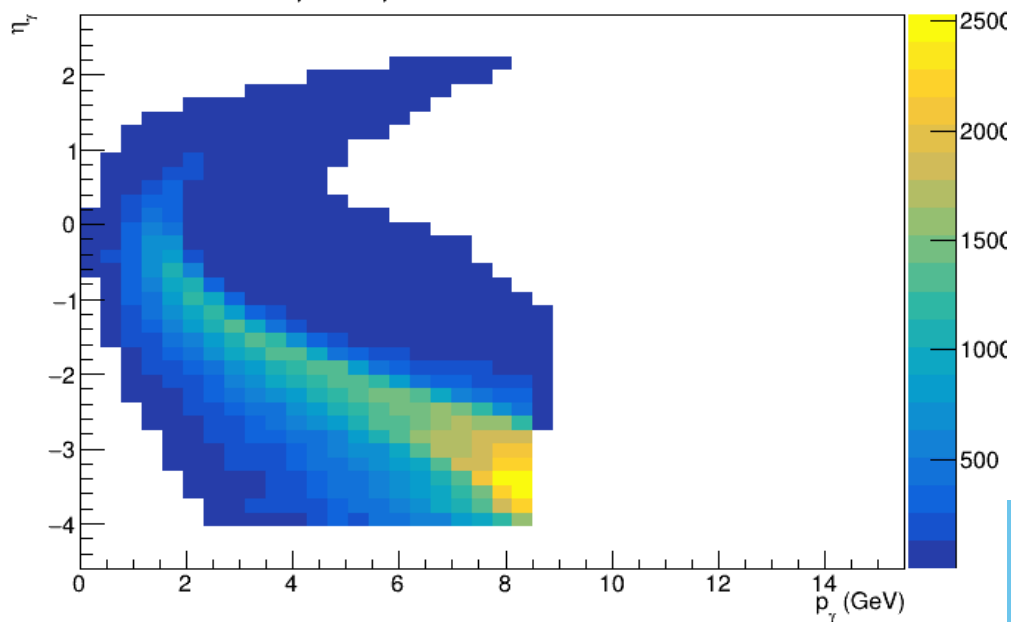
η_γ vs p_γ , $s=3 \times 20$, 10 fb⁻¹



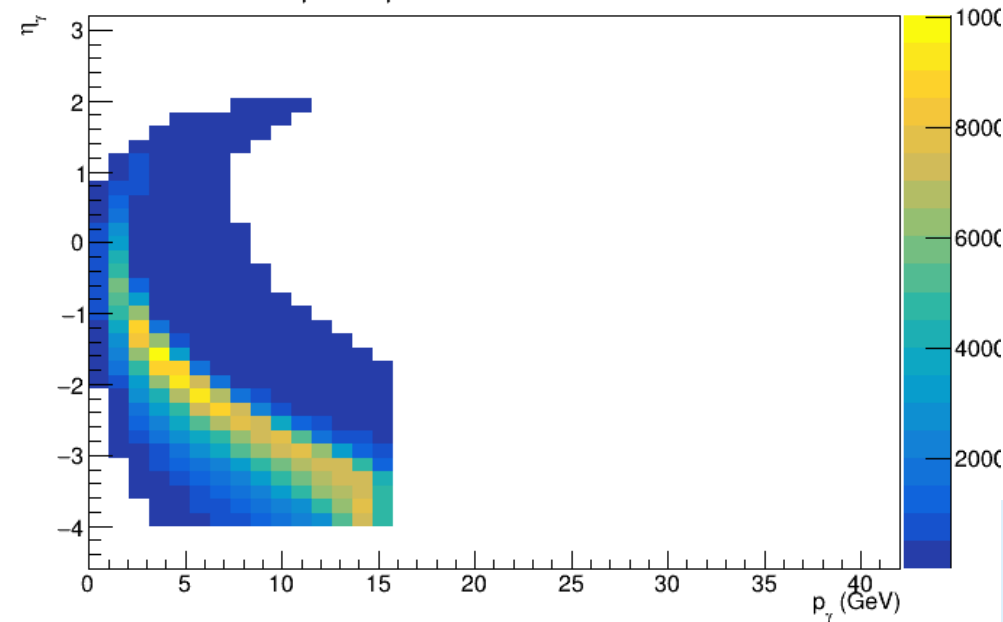
η_γ vs p_γ , $s=5 \times 41$, 10 fb⁻¹



η_γ vs p_γ , $s=10 \times 100$, 10 fb⁻¹

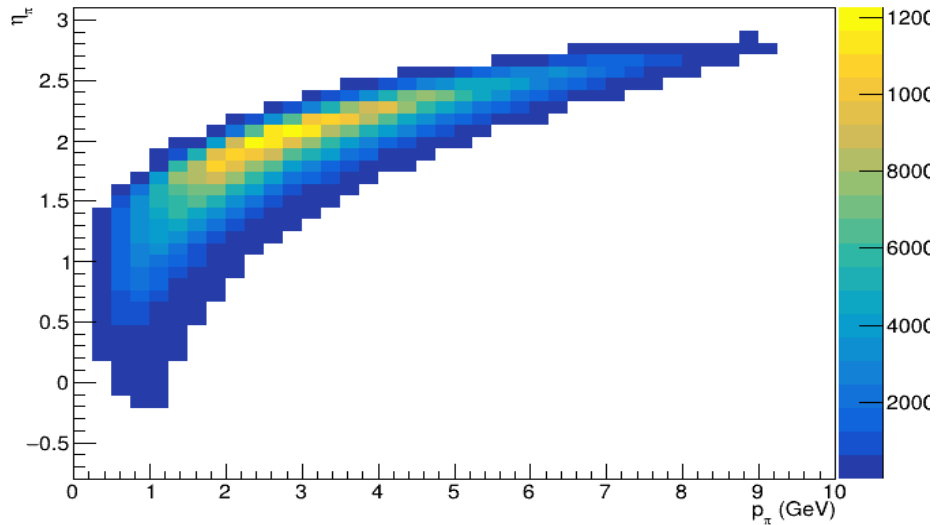


η_γ vs p_γ , $s=18 \times 275$, 10 fb⁻¹

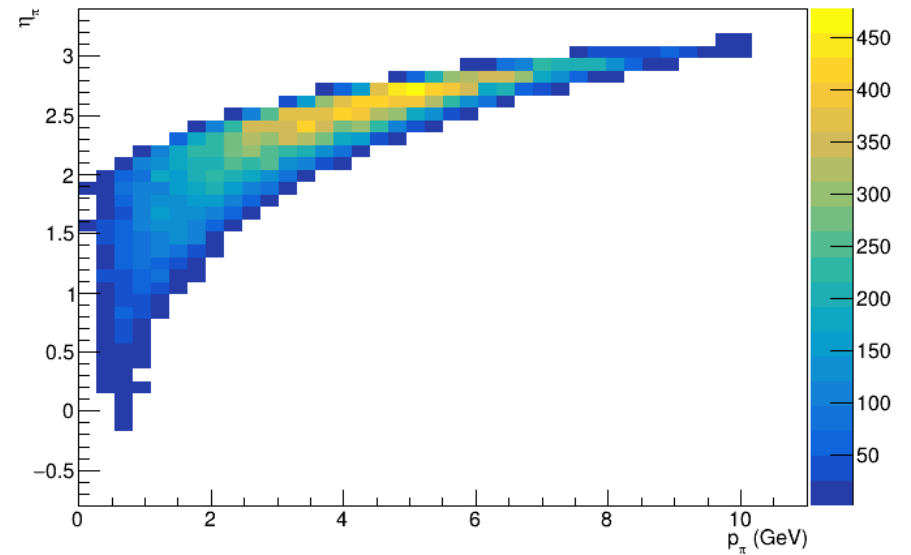


Recoil Pion distributions

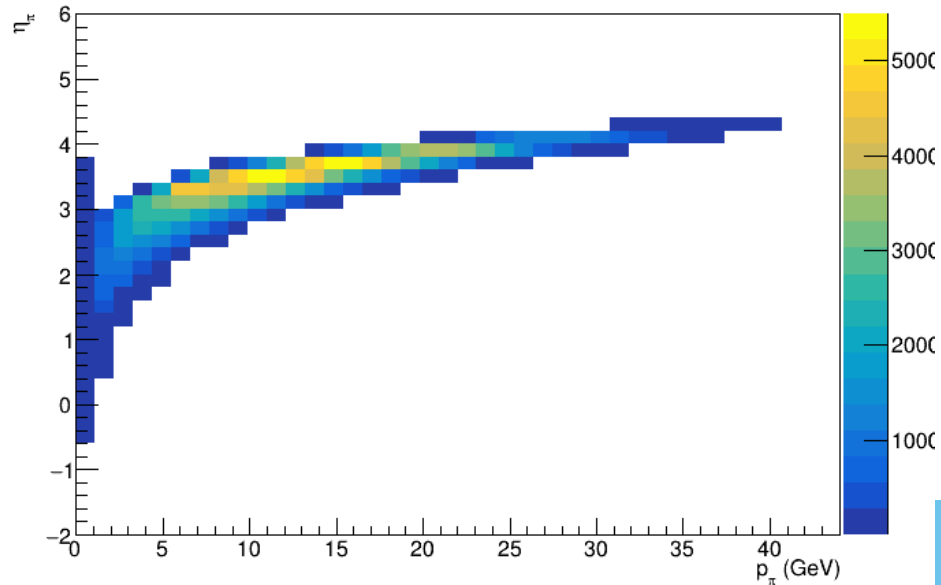
η_π vs p_π , $s=3 \times 20$, 10 fb⁻¹



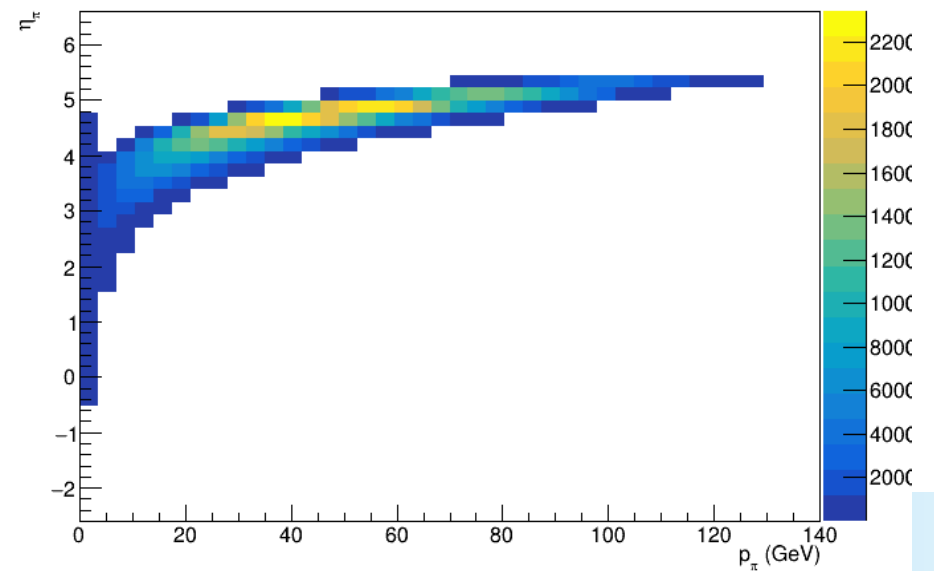
η_π vs p_π , $s=5 \times 41$, 10 fb⁻¹



η_π vs p_π , $s=10 \times 100$, 10 fb⁻¹

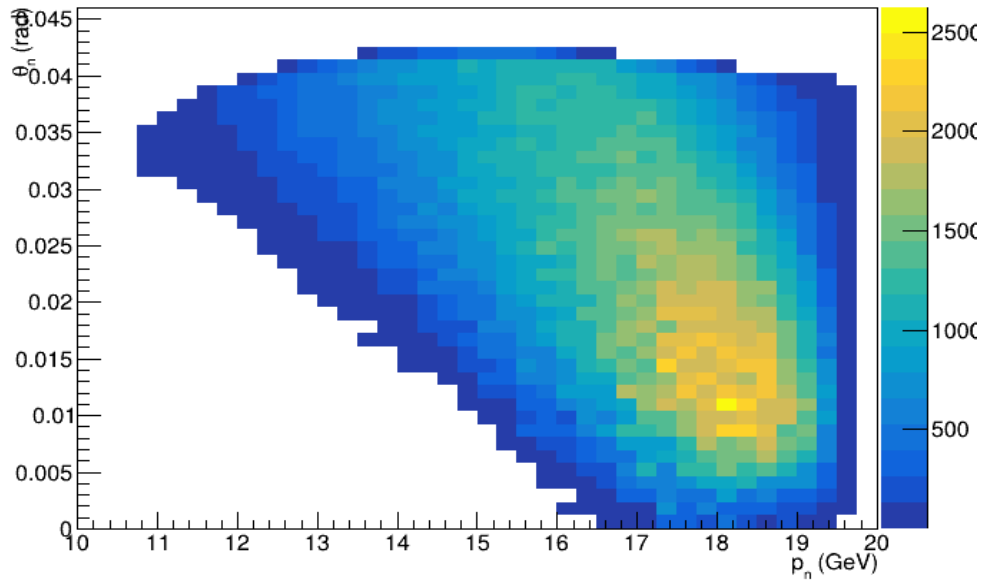


η_π vs p_π , $s=18 \times 275$, 10 fb⁻¹

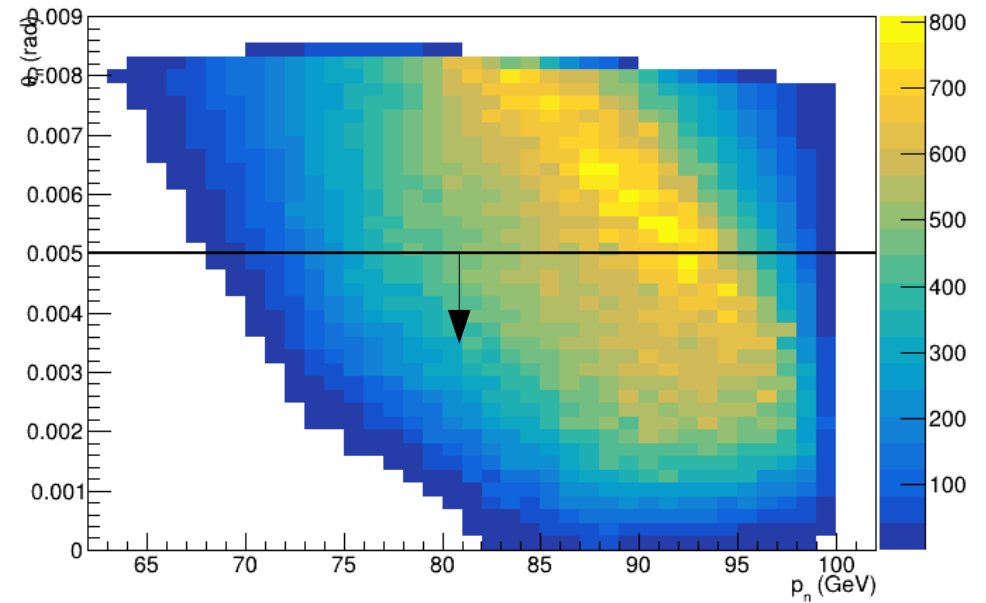


Neutron distributions

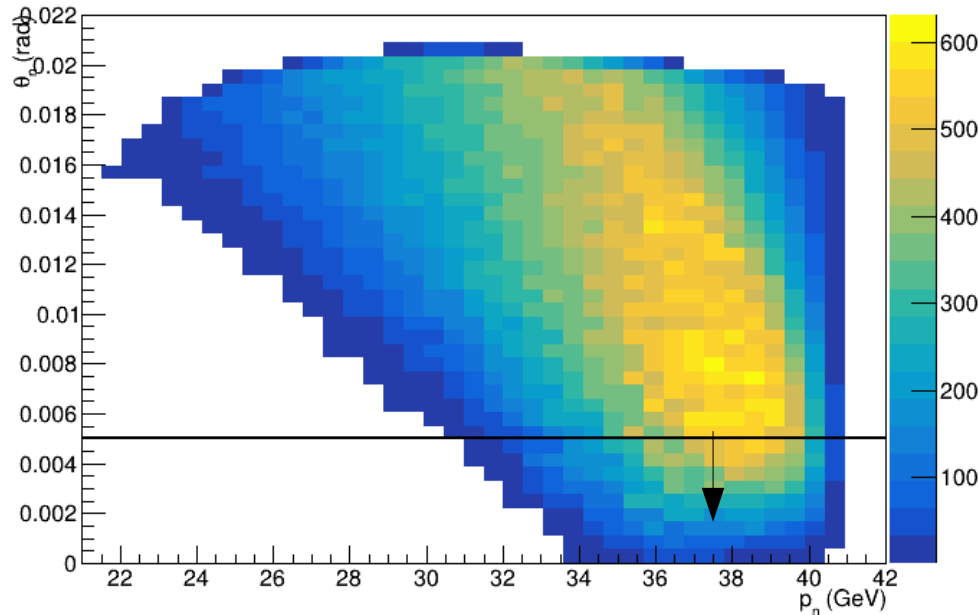
θ_n vs p_n , $s=3 \times 20$, 10 fb⁻¹



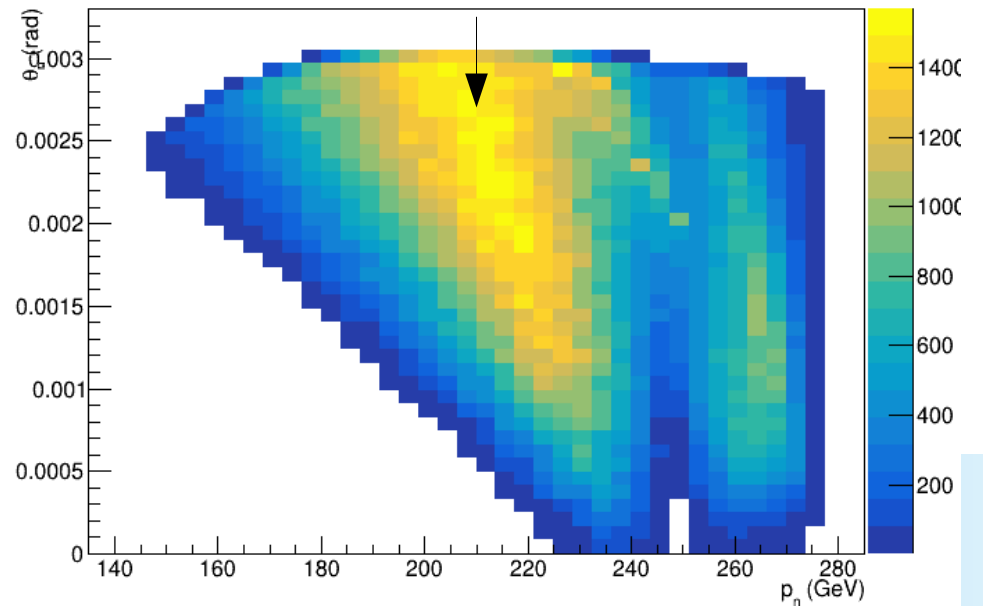
θ_n vs p_n , $s=10 \times 100$, 10 fb⁻¹



θ_n vs p_n , $s=5 \times 41$, 10 fb⁻¹

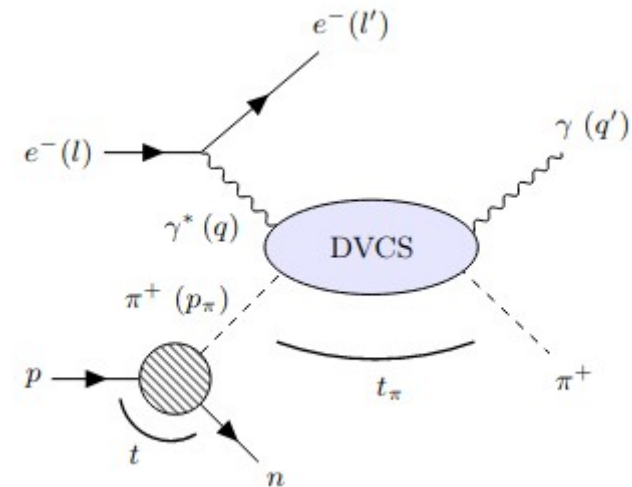
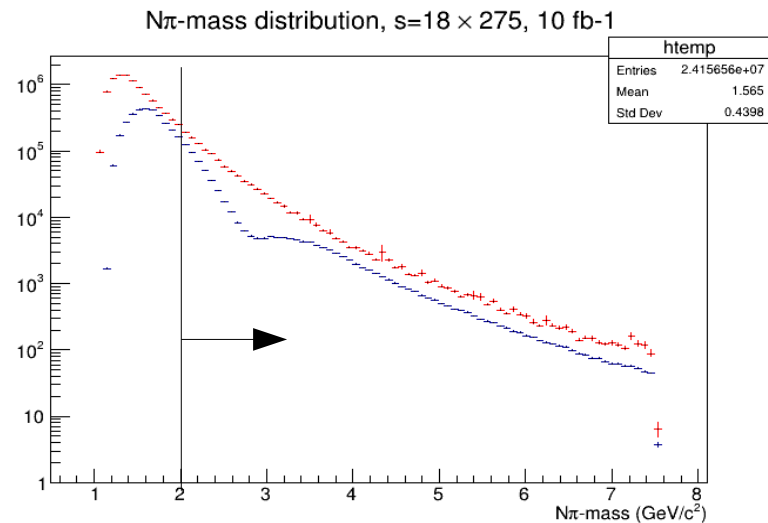


θ_n vs p_n , $s=18 \times 275$, 10 fb⁻¹



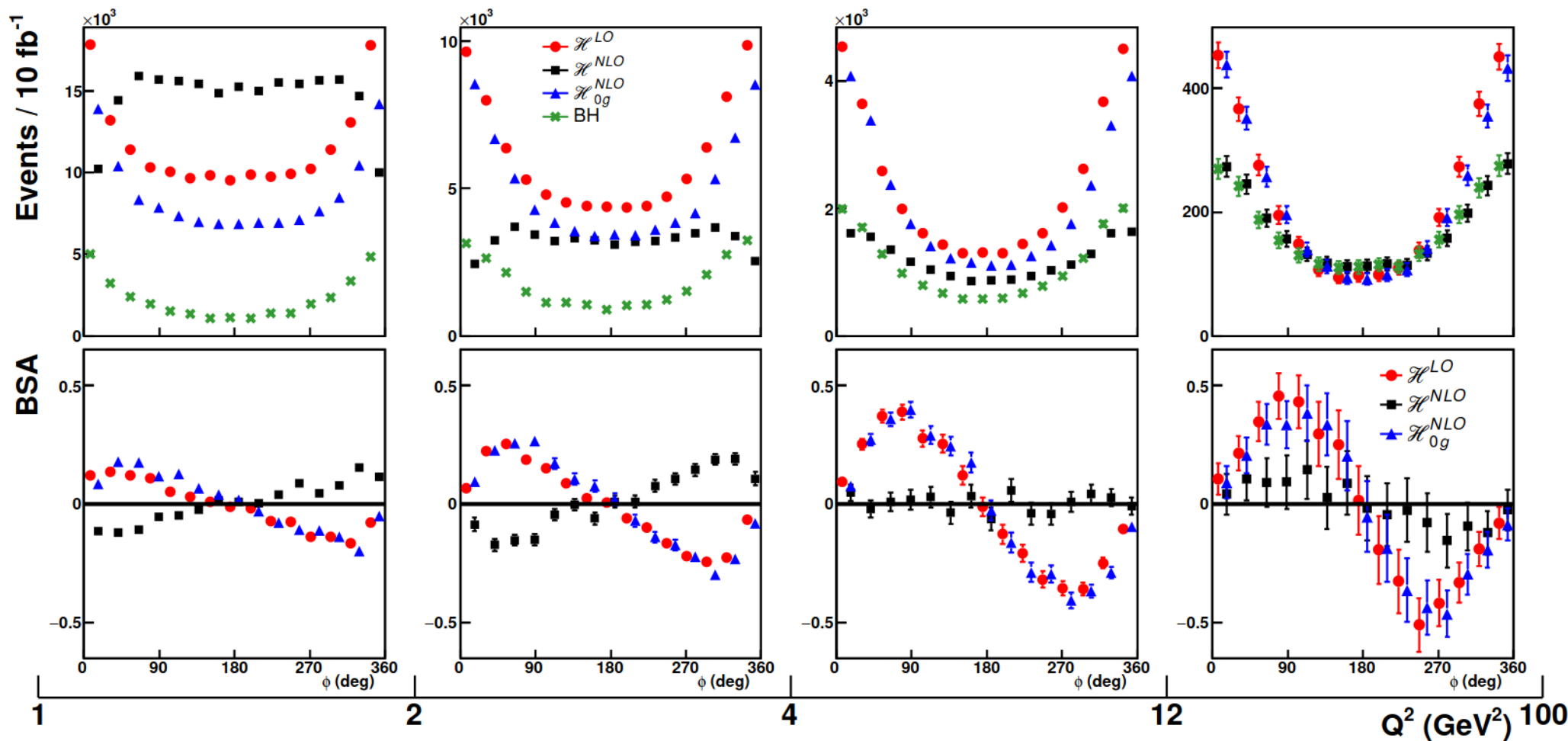
Sullivan process validity

- The invariant mass of the N-pion system must be greater than 2 GeV to avoid resonances contribution ($e p \rightarrow e \Delta \gamma$).



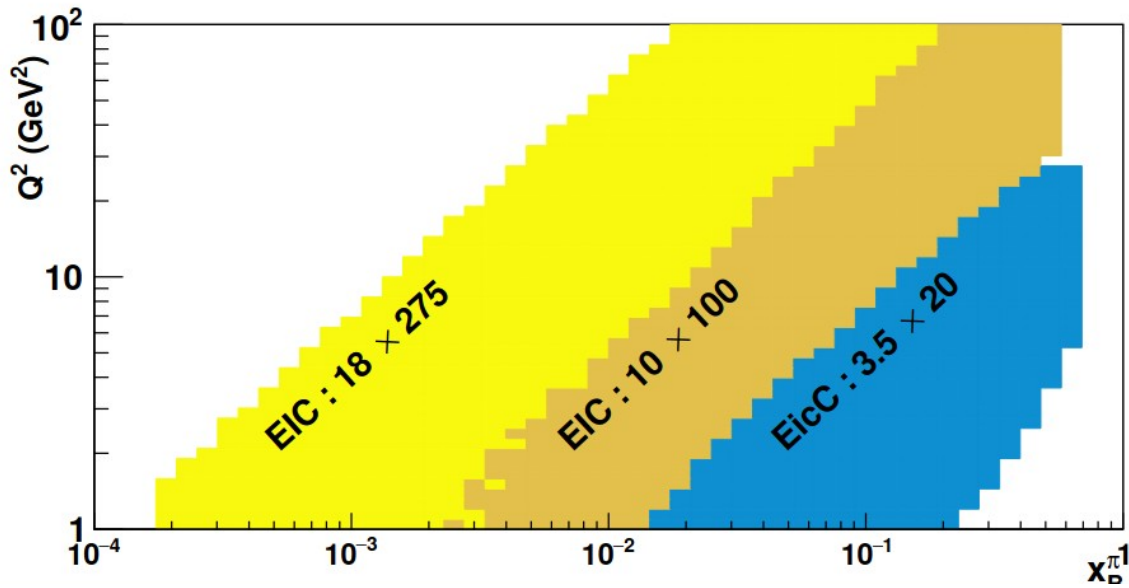
- Possible contribution from rho-to-pi but needs a model to evaluate them. The smaller the pion virtuality, the better.

Comparison for scenarii

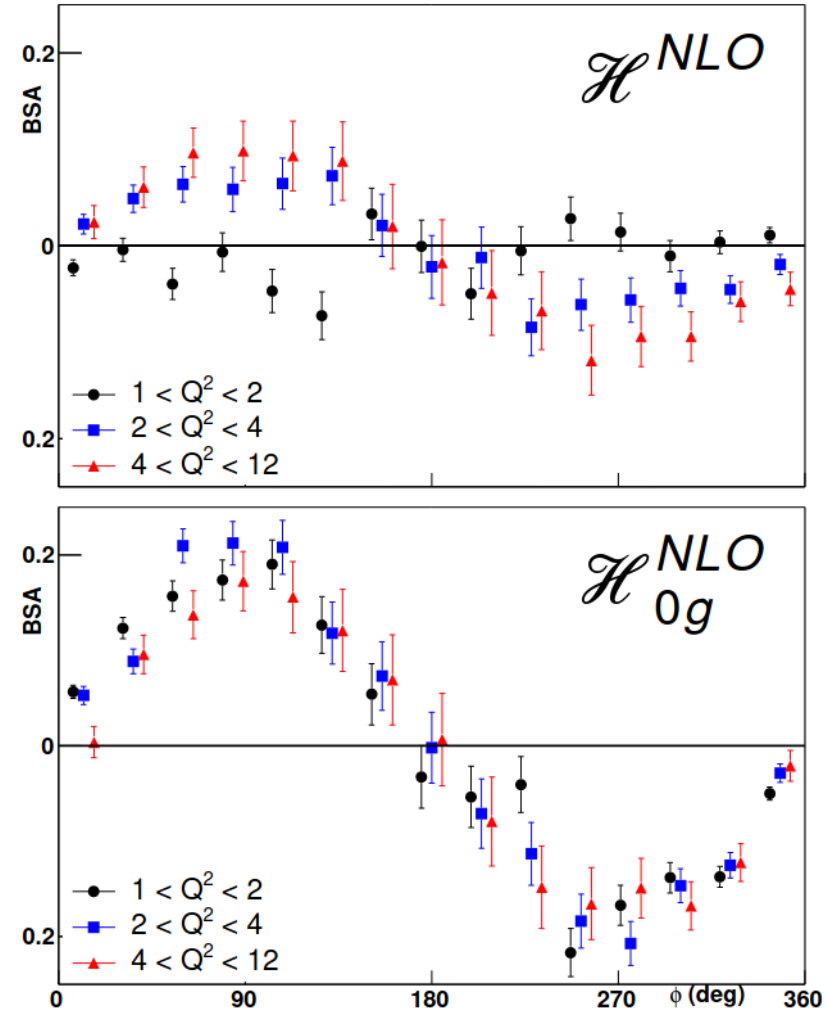


Glucos contributing negatively to the DVCS amplitude except at small Q^2 because of their number.

Gluons even in the valence



Even in the valence region at EIC, gluons can be spotted by a steep Q^2 – dependence of the asymmetry at low Q^2



What remains to be done...

- The process is definitely measurable. If the model is accurate, features in BSA could help us to pin down gluon dominance.
- Now, need to plug events in real EIC simulation to determine the resolution on the kinematical variables and use a more realistic acceptance.
- Refine the binning and perform t_{π} -scan studies.

More exclusive processes on pion

- Jose et al. provide us GPD models for both quarks and gluons in pion. From EIC measurements/simulation, would it be possible to retrieve the quark/gluon information from DVCS measurements ?
- What about DVMP (Phi-electroproduction) on the virtual pion ? Definitely helping to constrain gluonic content.
- Need to look into π^0 ... (Thank you Bernard)